Contents lists available at ScienceDirect

Physics Letters B

www.elsevier.com/locate/physletb

PHYSICS LETTERS B

CrossMark

On the momentum dependence of the flavor structure of the nucleon sea

Jen-Chieh Peng [a], Wen-Chen Chang [b], Hai-Yang Cheng [b], Tie-Jiun Hou [b], Keh-Fei Liu [c], Jian-Wei Qiu [d,e]

[a] *Department of Physics, University of Illinois at Urbana-Champaign, Urbana, IL 61801, USA*
[b] *Institute of Physics, Academia Sinica, Taipei 11529, Taiwan*
[c] *Department of Physics and Astronomy, University of Kentucky, Lexington, KY 40506, USA*
[d] *Physics Department, Brookhaven National Laboratory, Upton, NY 11973, USA*
[e] *C.N. Yang Institute for Theoretical Physics and Department of Physics and Astronomy, Stony Brook University, Stony Brook, NY 11794, USA*

ARTICLE INFO

ABSTRACT

Difference between the $\bar{u}$ and $\bar{d}$ sea quark distributions in the proton was first observed in the violation of the Gottfried sum rule in deep-inelastic scattering (DIS) experiments. The parton momentum fraction x dependence of this difference has been measured over the region $0.02 < x < 0.35$ from Drell–Yan and semi-inclusive DIS experiments. The Drell–Yan data suggested a possible sign-change for $\bar{d}(x) - \bar{u}(x)$ near $x \sim 0.3$, which has not yet been explained by existing theoretical models. We present an independent evidence for the $\bar{d}(x) - \bar{u}(x)$ sign-change at $x \sim 0.3$ from an analysis of the DIS data. We further discuss the x-dependence of $\bar{d} - \bar{u}$ in the context of meson cloud model and the lattice QCD formulation.

It is now a well established fact that the $\bar{u}$ and $\bar{d}$ distributions in the proton are strikingly different. The first evidence for this difference came from the observation of the violation of the Gottfried sum rule [1] in a deep-inelastic scattering (DIS) experiment by the NMC Collaboration [2]. The Gottfried sum rule, $I_G \equiv \int_0^1 [F_2^p(x_B) - F_2^n(x_B)]/x_B \, dx_B = 1/3$, is obtained under the assumption of a symmetric $\bar{u}$ and $\bar{d}$ sea [1], where x_B is the Bjorken variable and is effectively equal to parton momentum fraction x probed in DIS using the leading order QCD factorization formalism of the structure function $F_2(x_B)$. The NMC measurement of $I_G = 0.235 \pm 0.026$ implies that this assumption is invalid with an x-integrated difference of $\int_0^1 [\bar{d}(x) - \bar{u}(x)] dx = 0.148 \pm 0.039$.

The NMC result was subsequently checked using two independent experimental techniques. From measurements of the Drell–Yan cross section ratios of $[\sigma(p+d)]/[\sigma(p+p)]$, the NA51 [3] and the Fermilab E866 [4] experiments measured $\bar{d}/\bar{u}$ as a function of x over the kinematic range of $0.015 < x < 0.35$. As shown in Fig. 1, the $\bar{d}/\bar{u}$ ratios clearly differ from unity. From a semi-inclusive DIS measurement, the HERMES Collaboration also reported the observation [5] of $\bar{d}(x) - \bar{u}(x) \neq 0$, consistent with the Drell–Yan results.

The $\bar{d}(x)/\bar{u}(x)$ data obtained from the Drell–Yan experiments have provided stringent constraints for parameterizing the parton distribution functions (PDFs). Fig. 1 compares the data measured at $Q^2 = 54$ GeV^2 from Fermilab E866 with parameterizations of several PDFs. The E866 data show the salient feature that $\bar{d}/\bar{u}$ rises linearly with x for $x < 0.15$ and then drops as x further increases. At the largest value of x ($x = 0.315$), the $\bar{d}/\bar{u}$ ratio falls below unity, albeit with large experimental uncertainty. This intriguing x-dependence of $\bar{d}/\bar{u}$ is reflected in recent PDFs including CTEQ6 [6], CT10 [7], MSTW08 [8], and JR14 [9]. However, for the CTEQ4M [10] PDF, which predated the E866 data, the $\bar{d}/\bar{u}$ ratios at large x are not well described by the parameterizations. In particular, $\bar{d}(x)/\bar{u}(x)$ remains greater than unity, or equivalently, $\bar{d}(x) - \bar{u}(x) > 0$, at all x. The parameterizations of the more recent PDFs are sufficiently flexible to accommodate a sign-change for $\bar{d}(x) - \bar{u}(x)$ at $x \sim 0.3$, as suggested by the E866 data.

Many theoretical models have been put forward to explain the surprisingly large difference between $\bar{d}(x)$ and $\bar{u}(x)$. For reviews on various theoretical models, see Refs. [11–15]. While these models can explain the enhancement of $\bar{d}$ over $\bar{u}$ involving various mechanisms such as meson cloud, chiral-quark, intrinsic sea, soliton, and Pauli-blocking, none of them predicts that the $\bar{d}/\bar{u}$ ratio falls below unity at any value of x [14]. In order to understand the origin of the sea-quark flavor structure, it is important to improve the
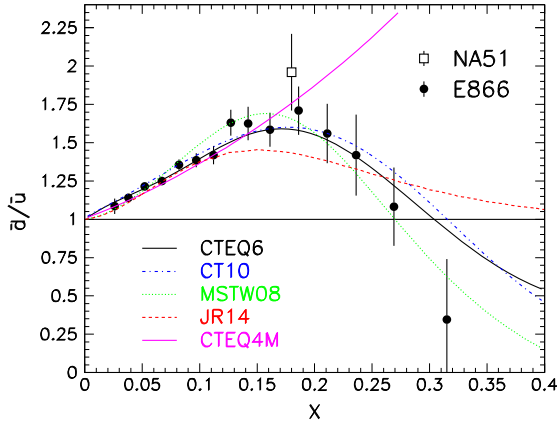
Fig. 1. Ratio of $\bar{d}(x)$ over $\bar{u}(x)$ versus Bjorken-x from experiments NA51 [3] and E866 [4]. Parameterizations from several parton distribution functions are also shown.

Fig. 2. Values of $\bar{d}(x) - \bar{u}(x)$ at $Q^2 = 4$ GeV^2 evaluated using Eq. (2), as discussed in the text. The open circles and filled stars correspond to results obtained with the JR14 and CT10 PDFs, respectively. Also shown are the values of $\bar{d}(x) - \bar{u}(x)$ at $Q^2 = 54$ GeV^2 from the Fermilab E866 experiment.

accuracy and to extend the kinematic coverage of the $\bar{d}/\bar{u}$ measurement to the $x > 0.3$ region. This is the goal of an ongoing Fermilab Drell–Yan experiment, E906 [16], and a proposed experiment [17] at the J-PARC facility. The x-dependence of $\bar{d}/\bar{u}$ (or the related quantity $\bar{d} - \bar{u}$) at large x remains a topics of much interest both theoretically and experimentally.

In this paper we address the intriguing possibility that $\bar{d} - \bar{u}$ changes sign at the $x \sim 0.3$ region. We first show that an independent experimental evidence for this sign-change, other than the one shown in Fig. 1 from the Drell–Yan data, comes from an analysis of the NMC DIS data. We then discuss the significance of this sign-change and the stringent constraint it imposes on theoretical models. We also discuss the implications on the x-dependence of $\bar{d} - \bar{u}$ using the lattice QCD formulation for the sea-quark parton distributions. Future measurements of $\bar{d}(x)/\bar{u}(x)$ at $x > 0.25$ in Drell–Yan experiments could provide strong constraints and new insights on the origins of the flavor structure of the proton's sea.

The NMC measurement of the Gottfried sum involves the F_2 structure functions on proton and neutron. In terms of QCD factorization, we have at the leading order in α_s,

$$F_2^p(x) - F_2^n(x) = \frac{1}{3}x\big[u(x) + \bar{u}(x) - d(x) - \bar{d}(x)\big], \qquad (1)$$

where $x = x_B$ was used at this order. Eq. (1) is obtained under the usual assumption of charge symmetry of parton distributions and the equality of heavy-quark (s, c, b) distributions in proton and neutron. Note that the Q^2 dependence in $F_2^{p,n}(x, Q^2)$ and parton distributions $q(x, Q^2)$ is implicit. The magnitude of order α_s^1 and α_s^2 perturbative QCD effect is estimated to be small, on the order of 0.2% at $Q = 10$ GeV [18]. From Eq. (1) and the definition of valence quarks, $u_v(x) = u(x) - \bar{u}(x)$ and $d_v(x) = d(x) - \bar{d}(x)$, one readily obtains the following expression:

$$\bar{d}(x) - \bar{u}(x) = \frac{1}{2}\big[u_v(x) - d_v(x)\big] - \frac{3}{2x}\big[F_2^p(x) - F_2^n(x)\big]. \qquad (2)$$

Eq. (2) shows that the x dependence of $\bar{d} - \bar{u}$ can be extracted from the NMC measurement of $F_2^p(x) - F_2^n(x)$ and the parametrization of $u_v(x) - d_v(x)$ from various PDFs. To illustrate this, we show in Fig. 2 the values of $\bar{d}(x) - \bar{u}(x)$ at $Q^2 = 4$ GeV^2 using Eq. (2), where the first term of the right-hand side, $u_v(x) - d_v(x)$, is taken from the NNLO JR14 parametrization [9] and the second term, $F_2^p(x) - F_2^n(x)$, is taken from the NMC data [2] at $Q^2 = 4$ GeV^2. The JR14 is a recent PDF where the nuclear corrections from the CJ group [19] is implemented and $\bar{d}(x) - \bar{u}(x) > 0$ is assumed at all x in the global analysis. We also show in Fig. 2 the values
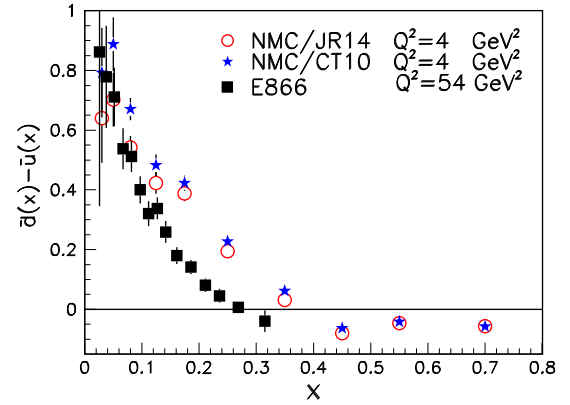
of $\bar{d}(x) - \bar{u}(x)$ at $Q^2 = 54$ GeV^2 (filled squares) derived by the E866 Collaboration [4]. The sign-change of $\bar{d} - \bar{u}$ at $x \sim 0.3$ as indicated by the E866 data is clearly consistent with the behavior of open circles obtained by using Eq. (2) based on the NMC data and the JR14 PDFs. Although the JR14 uses a parametrization of $\bar{d} - \bar{u}$ that is positive at all x, as shown in Fig. 1, we demonstrated in Fig. 2 that NMC data together with the valence quark distributions of JR14 could lead to a sign-change of $\bar{d}(x) - \bar{u}(x)$ distribution at $x \sim 0.3$. We have also performed calculations with other sets of recent PDFs, obtained very similar results and reached the same conclusion. In Fig. 2, we show, for example, the values of $\bar{d}(x) - \bar{u}(x)$ (filled stars) obtained by using $u_v(x) - d_v(x)$ of the CT10 PDF parametrization [7] along with the same NMC data. The values of $\bar{d}(x) - \bar{u}(x)$ obtained by using CT10 and JR14 are practically identical for $x > 0.2$. This finding is effectively a consequence of the fact that the $u_v(x) - d_v(x)$ distribution in Eq. (2) is well constrained by QCD global fit of the extensive DIS and hadronic scattering data.

Although Fig. 2 shows similar trends for the x-dependence of $\bar{d} - \bar{u}$ extracted from the E866 Drell–Yan and the NMC DIS data, these two data sets correspond to two different Q^2 scales. A more direct comparison can be obtained by analyzing the final results published by the NMC Collaboration on the ratio $R(x) = F_2^d(x)/F_2^p(x)$ [20]. The values of $F_2^p(x) - F_2^n(x)$ could be calculated from $2F_2^d(x) * (1/R(x) - 1/r_N^d(x))$, by using the parametrization of $F_2^d(x)$ of Ref. [21]. The $r_N^d(x)$ is the ratio of deuteron to isoscalar nucleon structure functions $F_2^d(x) = r_N^d(x) * (F_2^p(x) + F_2^n(x))/2$ and we use $r_N^d(x)$ of the CJ12mid set at $Q^2 = 100$ GeV^2 [22] for the evaluation. Refs. [20] and [21] included not only additional data that were not available for NMC's earlier evaluation of the Gottfried sum [2], but also the values of $R(x)$ at different bins of Q^2 ranging from 0.16 to 99.03 GeV^2. The high Q^2 data makes it possible to compare the E866 Drell–Yan data on $\bar{d}(x) - \bar{u}(x)$ at $Q^2 = 54$ GeV^2 with that evaluated using Eq. (2) and NMC data at a similar Q^2. As the E866 Drell–Yan data on $\bar{d}(x) - \bar{u}(x)$ correspond to $Q^2 = 54$ GeV^2, a comparison could be made by using the NMC data at similar Q^2. The mean values of Q^2 for the four highest Q^2 bins of NMC data are around 34, 45, 63, and 95 GeV^2. Fig. 3 shows $\bar{d}(x) - \bar{u}(x)$ for these four values of Q^2 using Eq. 2 with the JR14 parametrization of the valence quark distributions and the NMC data [20] for $F_2^p(x) - F_2^n(x)$. The uncertainties of both $R(x)$ and the parametrization of F_2^d have been included in the evaluation of $F_2^p(x) - F_2^n(x)$. Fig. 3 shows that the values of $\bar{d}(x) - \bar{u}(x)$ at $x > 0.3$ are mostly negative with the mean values of -0.009 ± 0.006, -0.012 ± 0.006, -0.016 ± 0.008, and -0.001 ± 0.008, respectively,
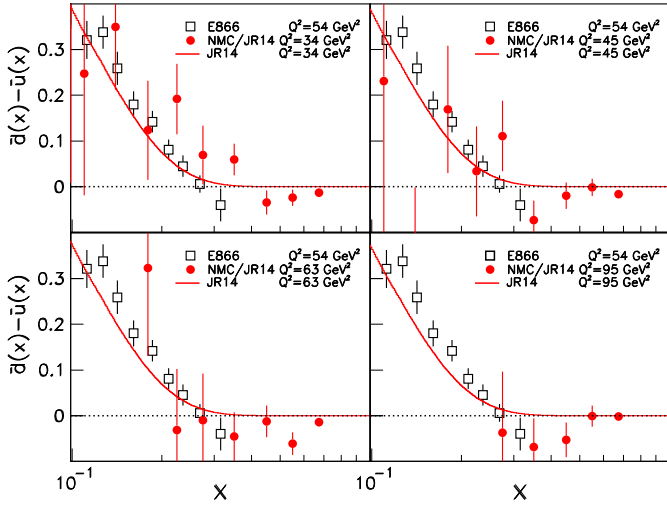
Fig. 3. Values of $\bar{d}(x) - \bar{u}(x)$ evaluated using Eq. (2) and the NMC data [20,21] of $R(x)$ and $F_2^d(x)$ at the four largest values of Q^2. The JR14 parametrization for $u_v(x) - d_v(x)$ at the corresponding Q^2 and the ratio of deuteron to isoscalar nucleon structure functions $r_N^d(x)$ of the CJ12mid set at $Q^2 = 100$ GeV^2 [22] are used. The values of $\bar{d}(x) - \bar{u}(x)$ from E866 measurement at $Q^2 = 54$ GeV^2 are also shown. The solid curves are $\bar{d}(x) - \bar{u}(x)$ from JR14.

for the four Q^2 bins. The agreement between the E866 and NMC results is now improved when compared with Fig. 2. In particular, both the NMC and the E866 experiments show evidence that $\bar{d}(x) - \bar{u}(x)$ changes sign at $x \sim 0.3$.

Since both the NMC data and the E866/NA51 Drell–Yan data are included in recent global fits for determining the parton distributions, it is conceivable that the NMC data have already played a role in constraining the behavior of $\bar{d}(x) - \bar{u}(x)$ at large x. Nevertheless, the possible sign-change of $\bar{d}(x) - \bar{u}(x)$ for $x \sim 0.3$ has only been attributed in the literature to the E866 data, which have large uncertainty at the highest x region. We show that an independent indication for this sign-change is already provided by the NMC DIS data, which were obtained prior to the E866 Drell–Yan data.

The significance of the sign-change of $\bar{d}(x) - \bar{u}(x)$ for $x > 0.3$, if confirmed by future experiments, is that it would severely challenge existing theoretical models which can successfully explain $\bar{d}(x) - \bar{u}(x)$ at $x < 0.25$, but predict no sign-change at higher x. Take for example the meson-cloud model [23–26], which treats proton as a linear combination of a bare proton plus pion–nucleon and pion–delta Fock states:

$$|p\rangle \rightarrow \sqrt{1 - a^2 - b^2}\, |p_0\rangle$$
$$+ a\left[-\sqrt{\frac{1}{3}}|p_0\pi^0\rangle + \sqrt{\frac{2}{3}}|n_0\pi^+\rangle \right]$$
$$+ b\left[\sqrt{\frac{1}{2}}|\Delta_0^{++}\pi^-\rangle - \sqrt{\frac{1}{3}}|\Delta_0^+\pi^0\rangle + \sqrt{\frac{1}{6}}|\Delta_0^0\pi^+\rangle \right]. \quad (3)$$

The subscript zeros denote bare baryons with flavor symmetric seas. The $\bar{u}$ and $\bar{d}$ seas have contributions from the valence antiquarks of the pion cloud, i.e., $\bar{d}$ in π^+ and $\bar{u}$ in π^-. The pion–nucleon amplitude is larger than the pion–delta amplitude ($a > b$) due to the heavier mass for the Δ. The excess of $\bar{d}$ over $\bar{u}$ arises because of the dominance of the $n_0\pi^+$ configuration over the less probable $\Delta_0^{++}\pi^-$ configuration. This leads to an overall excess of $\bar{d}$ over $\bar{u}$. Moreover, the x distribution for $\bar{u}$ is softer than that of $\bar{d}$, since π^- in the $\Delta_0^{++}\pi^-$ configuration carries a smaller fraction of the proton's momentum than π^+ in the $n_0\pi^+$ configuration. As a consequence, $\bar{d}(x) - \bar{u}(x)$ remains positive and does not change
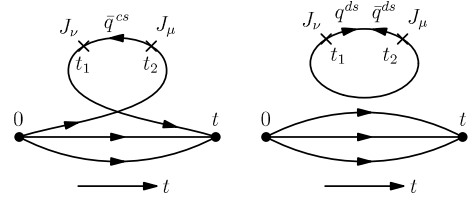

Fig. 4. Two gauge invariant and topologically distinct diagrams for (a) connected sea (left graph) and (b) disconnected sea (right graph).

sign at large x. The same conclusion can be obtained for the chiral quark model [27–29], in which the pions couple directly to the constituent quarks. Since there are two u quarks coupling to π^+ ($u \rightarrow \pi^+ + d$) and only one d quark coupling to π^- ($d \rightarrow \pi^- + u$), the larger probability for the π^+ meson cloud relative to the π^- cloud would lead to $\bar{d} > \bar{u}$ for all x. Similar conclusions can be obtained in the intrinsic sea model [30], the chiral-quark soliton model [31], and the statistical model [32].

To shed some light on the x-dependence of $\bar{d} - \bar{u}$, we consider the origins of sea quarks in the lattice QCD approach. There are two sources for the $\bar{d}$ and $\bar{u}$ seas in the path-integral formalism of the hadronic tensor defining the structure function $F_2(x)$ [33], as shown in the two gauge-invariant and topologically distinct diagrams in Fig. 4. One is the connected sea (CS) from the connected insertion diagram (Fig. 4(a)) and the other is the disconnected sea (DS) from the disconnected insertion diagram (Fig. 4(b)). For the case with isospin symmetry, i.e. $m_u = m_d$, it is shown [34] that the DS does not distinguish $\bar{u}$ from $\bar{d}$. Hence, the $\bar{u}(x), \bar{d}(x)$ difference must originate solely from the CS (Fig. 4(a)). It is well known that sea quark distribution generated by the disconnected diagram is a steeply falling function of momentum fraction x, because the gluon radiated from the initial quark line is dominantly soft due to the $\propto 1/x$ behavior of the splitting kernel. In contrast, sea quarks generated by the connected diagram have an $x^{-1/2}$ behavior at small x and are most relevant in the medium and large x region. While lattice QCD so far could only generate the moments rather than the x-dependence of quark distributions, a first attempt to separate the CS and DS components of the $\bar{u}(x) + \bar{d}(x)$ was reported recently [35]. The extracted CS and DS for $\bar{u}(x) + \bar{d}(x)$ [35] have a distinct x dependence in qualitative agreement with expectation. The DS dominates the small x region (i.e. $x < 0.05$) while the CS dominates the $x > 0.05$ region.

It is instructive to consider $\bar{d}(x) - \bar{u}(x)$ in three different x regions. At small x, the DS with small x behavior of x^{-1} dominates. For $Q^2 = 2.5$ GeV^2 where the CS and DS are explicitly separated [35], this is the region where $x < 0.05$. Since the only difference between $\bar{u}^{DS}$ and $\bar{d}^{DS}$ is the u/d mass difference which is much smaller than the scale for the validity of the parton picture, we expect the difference between them due to isospin symmetry breaking to be very small. In the mid-x region (from $x = 0.05$ to $x \sim 1/3$), dominated by the CS with an x-dependence of $x^{-1/2}$, the Fock space wavefunction of the quarks in the nucleon is important. It is in this region that the DIS and Drell–Yan experiments reveal that $\bar{u}(x) < \bar{d}(x)$. The dominance of the CS at this region of x suggests a greater chance for the CS partons to share the momentum with the valence quarks resulting in the meson–baryon configurations. Hence the pronounced feature of $\bar{u}(x) < \bar{d}(x)$ in this x region can be understood in terms of the pion cloud model.

At even larger x ($x > 1/3$) the nature of the sea quarks is expected to be strongly influenced by the valence quarks. Intuitively, the connected sea diagram provides a natural mechanism for generating more $\bar{u}(x)$ than $\bar{d}(x)$ at this region, since there are two u valence quarks capable of generating $\bar{u}$ quarks as shown in Fig. 4. Fig. 5 shows specific examples of diagrams responsible for generating antiquarks from one (top) or two (bottom) valence quarks.
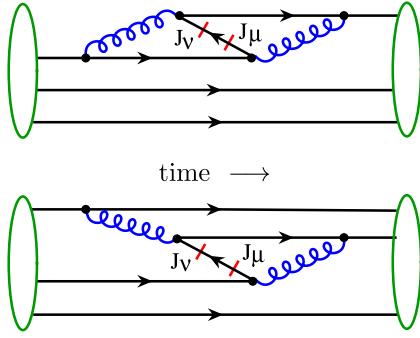
Fig. 5. QCD quantum fluctuation capable of generating connected $\bar{u}(x)$ or $\bar{d}(x)$, involving one (top) or two (bottom) valence quarks, which could lead to more $\bar{u}(x)$ than $\bar{d}(x)$.

In Fig. 5, the antiquark mode of the QCD quantum fluctuation of a quark is probed by the currents J_μ and J_ν. The quantum fluctuation could be thought as a time sequence of four steps: 1) fluctuation of a valence quark into a quark and a highly virtual gluon, 2) a quick splitting of the gluon into a quark and antiquark pair, 3) annihilation or recombination of the quark and the newly produced antiquark into a highly virtual gluon, which is then, 4) absorbed by the quark. Since both valence u and d quarks can go through the same QCD quantum fluctuation to generate $\bar{u}$ and $\bar{d}$ quarks, the mechanism depicted in Fig. 5 could generate about twice of $\bar{u}(x)$ over $\bar{d}(x)$ due to the 2-to-1 ratio of valence quarks. But, this fluctuation is the most probable only if partons involved have an excellent coalescence, and therefore, it should be very short-lived. That is, it is unlikely to generate enough imbalance between $\bar{u}$ and $\bar{d}$ to compete with what could be generated by the pion cloud or other mechanisms/models at small-x. However, this mechanism is not very sensitive to the parent quark's momentum fraction x, and would become relevant when the imbalance generated by other mechanisms/models dies away at large x. It is noted that $\bar{u} > \bar{d}$ was also suggested by a model calculation examining the antisymmetrization effect of the nucleon sea arising from gluon exchange between confined valance quarks [36]. The data indicates that such transition takes place at $x \sim 1/3$. A detailed calculation of $\bar{u}(x)$ and $\bar{d}(x)$ in terms of connected (or recombination) diagrams, like that in Ref. [37], is beyond the scope of this letter, and will be presented later.

In summary, we have discussed the importance of the possible sign-change for $\bar{d}(x) - \bar{u}(x)$ at $x \sim 0.3$ for understanding the flavor structure of the nucleon sea. We present an independent evidence for the $\bar{d}(x) - \bar{u}(x)$ sign-change at large x from an analysis of existing DIS data. This sign-change cannot be explained by any existing theoretical model on the nucleon sea. Nevertheless, a qualitative explanation for the sign-change at large x is provided in the context of lattice QCD formalism. Up to now, only the connection between the NMC data and the integral of $\bar{d}(x) - \bar{u}(x)$ has been discussed. The current work hopefully would lead to some dedicated studies by the various PDF groups to assess the impact of the NMC data on the x-dependence of $\bar{d} - \bar{u}$. We note that $\bar{d}(x) - \bar{u}(x)$ can be calculated on the lattice [33] from the structure function of the hadronic tensor or the recently proposed direct calculation via a Lorentz boost [38,39]. When reliable results are obtained, they would provide a direct check on the possible sign-change for $\bar{d}(x) - \bar{u}(x)$ at $x \sim 0.3$. New experimental information on the x-dependence of the $\bar{d} - \bar{u}$ at large x, anticipated for future Drell–Yan experiments, together with comprehensive global analyses would be critical for understanding the origins of the flavor structure of the nucleon sea.

References

[1] K. Gottfried, Phys. Rev. Lett. 18 (1967) 1174.
[2] A. Amaudruz, et al., NMC Collaboration, Phys. Rev. Lett. 66 (1991) 2712;
    M. Arneodo, et al., Phys. Rev. D 50 (1994) R1.
[3] A. Baldit, et al., NA51 Collaboration, Phys. Lett. B 332 (1994) 244.
[4] E.A. Hawker, et al., E866/NuSea Collaboration, Phys. Rev. Lett. 80 (1998) 3715;
    J.C. Peng, et al., Phys. Rev. D 58 (1998) 092004;
    R.S. Towell, et al., Phys. Rev. D 64 (2001) 052002.
[5] K. Ackerstaff, et al., HERMES Collaboration, Phys. Rev. Lett. 81 (1998) 5519.
[6] H.L. Lai, et al., J. High Energy Phys. 0704 (2007) 089.
[7] H.L. Lai, et al., Phys. Rev. D 82 (2010) 074024.
[8] A.D. Martin, W.J. Stirling, R.S. Thorne, G. Watt, Eur. Phys. J. C 63 (2009) 189.
[9] P. Jimenez-Delgado, E. Reya, Phys. Rev. D 89 (2014) 074049.
[10] H.L. Lai, et al., Phys. Rev. D 55 (1997) 1280.
[11] J.P. Speth, A.W. Thomas, Adv. Nucl. Phys. 24 (1998) 83.
[12] S. Kumano, Phys. Rep. 303 (1998) 183.
[13] R. Vogt, Prog. Part. Nucl. Phys. 45 (2000) 105.
[14] G.T. Garvey, J.C. Peng, Prog. Part. Nucl. Phys. 47 (2001) 203.
[15] J.C. Peng, J.-W. Qiu, Prog. Part. Nucl. Phys. 76 (2014) 43.
[16] Fermilab E906 proposal, Spokespersons: D. Geesaman and P. Reimer.
[17] J-PARC P04 Proposal, Spokespersons: J.C. Peng and S. Sawada.
[18] A.L. Kataev, G. Parenteb, Phys. Lett. B 566 (1983) 97.
[19] A. Accardi, W. Melnitchouk, J.F. Owens, M.E. Christy, C.E. Keppel, L. Zhu, J.G. Morfin, Phys. Rev. D 84 (2011) 014008.
[20] M. Arneodo, et al., NMC Collaboration, Nucl. Phys. B 487 (1997) 3.
[21] M. Arneodo, et al., NMC Collaboration, Phys. Lett. B 364 (1995) 107.
[22] J.F. Owens, A. Accardi, W. Melnitchouk, Phys. Rev. D 87 (2013) 094012.
[23] A.W. Thomas, Phys. Lett. B 126 (1983) 97.
[24] E.M. Henley, G.A. Miller, Phys. Lett. B 251 (1990) 453.
[25] S. Kumano, J.T. Londergan, Phys. Rev. D 44 (1991) 717.
[26] W.P. Hwang, J. Speth, G.E. Brown, Z. Phys. A 339 (1991) 383.
[27] E. Eichten, I. Hinchliffe, C. Quigg, Phys. Rev. D 45 (1992) 2269.
[28] T.P. Cheng, L.F. Li, Phys. Rev. Lett. 74 (1995) 2872.
[29] A. Szczurek, A. Buchmans, A. Faessler, J. Phys. C 22 (1996) 1741.
[30] W.C. Chang, J.C. Peng, Phys. Rev. Lett. 106 (2011) 252002;
    W.C. Chang, J.C. Peng, Phys. Lett. B 704 (2011) 197.
[31] P.V. Pobylitsa, et al., Phys. Rev. D 59 (1999) 034024.
[32] C. Bourrely, J. Soffer, Phys. Rev. D 51 (1995) 2108.
[33] K.F. Liu, Phys. Rev. D 62 (2000) 074501.
[34] K.F. Liu, S.J. Dong, Phys. Rev. Lett. 72 (1994) 1790.
[35] K.F. Liu, W.C. Chang, H.Y. Cheng, J.C. Peng, Phys. Rev. Lett. 109 (2012) 252002.
[36] F.M. Steffens, A.W. Thomas, Phys. Rev. C 55 (1997) 900.
[37] F.E. Close, J.-W. Qiu, R.G. Roberts, Phys. Rev. D 40 (1989) 2820.
[38] X. Ji, Phys. Rev. Lett. 110 (2013) 262002.
[39] H.W. Lin, et al., arXiv:1402.1462.